International Journal of Geosynthetics and Ground Engineering (2020) 6:15
https://doi.org/10.1007/s40891-020-00201-6

ORIGINAL PAPER

On the Response of Polyethylene Pipes to Lateral Ground Movements: Insights from Finite-Discrete Element Analysis

Masood Meidani[1] · Mohamed A. Meguid[1] · Luc E. Chouinard[1]

Received: 9 February 2020 / Accepted: 10 May 2020

Abstract
The current knowledge of the behaviour of polyethylene pipes subjected to lateral soil movement is limited and the commonly used design equations were initially developed for steel pipes. In this study, an attempt has been made to understand the soil–structure interaction using a three-dimensional finite-discrete (FE-DE) element model of a medium density polyethylene (MDPE) pipe buried in dense sand and subjected to lateral soil movement. The soil particles are modelled using discrete elements, while the pipe is modelled using finite elements and interface elements are introduced to transfer the forces between the two domains. Validation is performed using experimental data. This study shows that, when a pipe section experiences lateral movement induced by two symmetrically applied loads, the pipe will resist the imposed lateral forces by bending. Particle displacement patterns show that passive wedges develop locally close to the applied loads and the remaining pipe sections experience negligible deformation. Furthermore, it is found that the current expressions used to estimate the ultimate lateral soil force on buried pipes in granular soil, which is generally developed for rigid steel pipes, should be used with caution as they may overestimate the soil load on flexible MDPE pipes.

Keywords Pipe–soil interaction · Coupled analysis · Flexible pipes · Ground movement

Introduction

Buried pipes are widely used for transporting oil, gas and other water. Natural Resources Canada [1] reports that there are more than 800 thousand kilometres of transmission and distribution pipelines in Canada. Considering the significant benefits of pipelines to the economy, these infrastructures are considered as critical lifelines. Only in 2014, Canada has spent $1.5 billion on pipeline monitoring and maintenance to ensure public safety; however, the Transportation Board of Canada reported more than 1200 pipeline incidents occurred in Canada over the past 10 years. Part of these incidents are related to material corrosion, excavation damage or incorrect operation; however, permanent ground displacement (PGD) was found to be a major factor that causes pipeline failure. Permanent ground movements due to earthquakes, slope movements and landslides can impose unequal lateral displacements on the pipe and the surrounding soil leading to axial and flexural strains in pipe structure.

The levels of pipe stresses and strains caused by PGD are function of: (i) the relative displacement between the soil and the buried pipe; (ii) the spatial distribution of the PGD; (iii) the extent of the pipe section experiencing ground movement; and (iv) the direction of the ground movement relative to the axis of the pipe. For example, if the ground movement is parallel to the pipe axis (Longitudinal PDG), axial forces are imposed on the pipe and the pipe experiences only axial strains. In contrast, if the direction of the pipeline is perpendicular to the direction of ground movement (Lateral PGD), then both axial and flexural strains are generated within the pipe. In the past five decades, research has been conducted to study pipe–soil interaction using theoretical, experimental and numerical methods [e.g., 2–8]. While experimental studies are useful and allow for the load–displacement relationship to be investigated, numerical approaches are more suitable to investigate the response of both the pipe and the backfill soil.

✉ Mohamed A. Meguid
mohamed.meguid@mcgill.ca

Masood Meidani
masood.meidani@mail.mcgill.ca

Luc E. Chouinard
luc.chouinard@mcgill.ca

[1] McGill University, Montreal, Canada

Published online: 22 May 2020

Finite-element method (FEM) has been widely used to investigate soil–pipe interaction problems [9–13]. For example, Roy et al. [11] conducted a series of finite element analyses on pipelines buried in dense sand subjected to lateral soil movement. The analysis was performed under two-dimensional plane strain condition adopting the modified Mohr–Coulomb failure model. While the continuum-based FE method is capable of analysing soil behaviour at the macroscopic scale, it is challenging to consider particles discontinuity and capture their response at the microscale level. The discrete element method (DEM) is an alternative approach to study this class of problems. The method was introduced by Cundall and Strack [14] and has been used by several researchers [e.g., 15, 16] to study various soil–structure interaction problems. Meidani et al. [17] performed a large-scale three-dimensional discrete element analysis on a rigid steel pipe buried in dense sand to evaluate the response of the pipe under relative axial ground movement. Although the discrete element method is a promising approach to capture the discontinuous nature of granular material [18], modeling structural components using bonded discrete particles [19] may lead to inaccurate prediction of strains and stresses within the structural elements. This has been attributed to the inflexibility of the bonded particles particularly when modeling flexible pipes. Coupling the discrete and finite element approaches is a possible solution that takes advantage of both methods. Several algorithms have been proposed for transferring the loads and displacements between the discrete and finite elements [15, 20, 21]. Dang and Meguid [22] developed a hybrid FE-DE method to solve soil–structure interaction problems involving large deformations. They introduced interface elements between the two domains such that the forces are transferred between the discrete particles and the nearby finite-element nodes. Tran et al. [23] and [24] employed this technique to study other soil–structure interaction problems.

In this research, a coupled FE-DE method is used to evaluate the response of MDPE pipe installed in dense granular material and subjected to lateral movement. Emphasis is placed on the bending behaviour of the pipe and the response of the surrounding soil. The backfill material is modelled using discrete particles, whereas the MDPE pipe is created using finite elements. A triaxial test is numerically simulated to determine the micro parameters needed to represent the response of the discrete particles under different confining pressures. The model is then used to explore the response of the MDPE pipe to lateral soil movement and the results are validated using experimental data. The detailed behaviour of the pipe and the backfill soil such as strains, stresses and particle displacement patterns is investigated. Finally, the available design guidelines such as [25] used to calculate lateral loads on buried pipes are evaluated.

Soil–Pipe Interaction

Plastic polyethylene (PE) pipes are commonly used in natural gas distribution networks. Although extensive research has been previously conducted on buried pipes subjected to ground movement, it was mostly limited to steel pipelines. Hence, the solutions developed for steel pipes are usually recommended in guidelines [25] to evaluate the response of PE pipes. This may result in inaccurate estimates of forces due to the difference in stiffness between polyethylene and steel pipes.

The current approach that is commonly used to calculate the soil resistance to transverse pipe movement is based on a bilinear relationship [26], as shown in Fig. 1, such that

$$F_{\mathrm{L}} = K_{\mathrm{L}} \times \left(U_{\mathrm{P}} - \delta_{\mathrm{P}}\right), \tag{1}$$

where F_{L} is the soil resistance; K_{L} is the soil modulus; U_{P} is the pipeline lateral displacement and δ_{P} is the soil lateral movement. The response is considered to be linear elastic before the relative displacement exceeds its limiting value (D_{p}). The equation used to calculate the ultimate soil resistance on a buried pipe is expressed as follows:

$$P_{\mathrm{u}} = \gamma \times H \times N_{\mathrm{q}} \times D \tag{2}$$

where P_{u} is the peak soil lateral resistance; H is pipe burial depth; D is diameter of pipe and N_{q} is a dimensionless force factor. It is noted that N_{q} is function of H/D ratio and soil friction angle and is generally estimated using design charts proposed by different researchers. For instance, the chart for N_{q} recommended by ASCE [27] is based on the work of O'Rourke [28], whereas the American Lifeline Alliance [25] recommends a different chart that is based on Hansen [29].

A schematic diagram that shows a simplified version of the soil–pipe interaction under lateral ground movement is

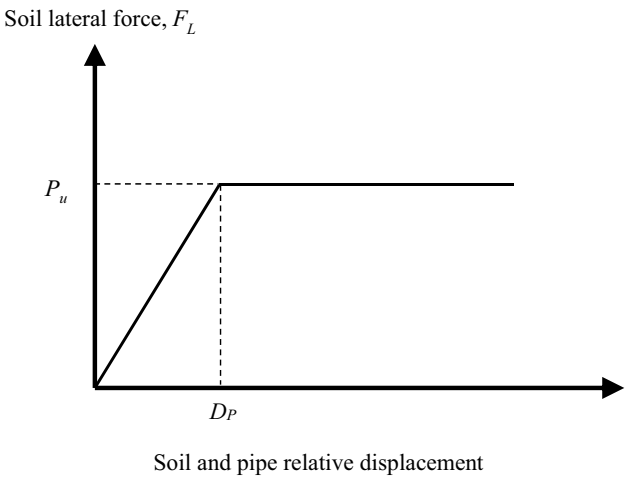

Fig. 1 Relationship between soil resistance and relative displacement

presented in Fig. 2. The soil in region 1 is relatively stable with minimum relative displacement between the pipe and the soil with curvature that is opposite to the direction of the soil movement. In regions 2 and 3, the relative displacement increases and the curvature changes to a direction opposite to the soil movement. Finally, in region 4, the pipe curvature decreases towards the centre of the pipe section and becomes zero at the centreline.

The induced lateral force on the pipeline is generally resisted by combination of bending and axial strains. Early analytical studies on the response of pipes subjected to lateral soil loading assumed that only bending strains resists the applied soil force. However, this assumption is only valid for pipe sections under small relative displacements, where the stresses remain within the elastic range. For large relative displacements, the pipe section deforms under axial loads and the axial strains carry most of the soil load [6]. It has been reported [30] that pipe sections close to the boundary between the stable and unstable soil (regions 2 and 3 in Fig. 2) bear the soil load via a combination of bending and axial strains, whereas the remaining section (region 4) carry soil forces entirely by bending. In this study, only sections of the pipeline that carry loads by bending (region 4) are investigated and the equations used to calculate the peak lateral forces are reviewed (Fig. 2).

Coupled Finite-Discrete Element Framework

The code used in this study is based on that of Dang and Meguid [22, 31] who developed a coupled 3D FE-DE framework by implementing an algorithm into an open source discrete element program YADE [32, 33].

Interface elements are introduced in the framework to transfer the contact forces from finite elements to discrete particles and vice versa. The interfaces are triangular shaped elements generated using finite element to represent the exact surface of the complex structure. As hexahedral shapes are used for the FE, a contact face is divided into four triangles by generating a new node at the centre using Eq. 3:

$$X^{(\mathrm{O})} = \frac{1}{4}\sum_{i=1}^{4} X^{(i)}, \tag{3}$$

where $X^{(i)}$ is the coordinate of node i of the hexahedral element. Figure 3 presents a schematic of the interaction between DE, FE and interface elements. The contact law governing the interaction between the interface elements and the discrete particles is the same as the particle–particle contact law discussed in the previous section. The normal and tangential overlap between the interface and the particle is calculated and the normal and tangential forces are determined using the procedure detailed by Meidani et al. [8]. The total contact force ($\vec{F}_{\mathrm{contact}} = \vec{F}_{\mathrm{N}} + \vec{F}_{\mathrm{T}}$) is computed and Eq. (4). is then employed to calculate the forces transmitted to the FE nodes. Details of the coupled algorithm are provided by Dang and Meguid (2010, 2013):

$$\vec{F}_i = \vec{F}_{\mathrm{contact}}.N_i = \left(\vec{F}_{\mathrm{N}} + \vec{F}_{\mathrm{T}}\right).N_i \tag{4}$$

where N_i is the shape function calculated using the natural coordinates of the contact point.

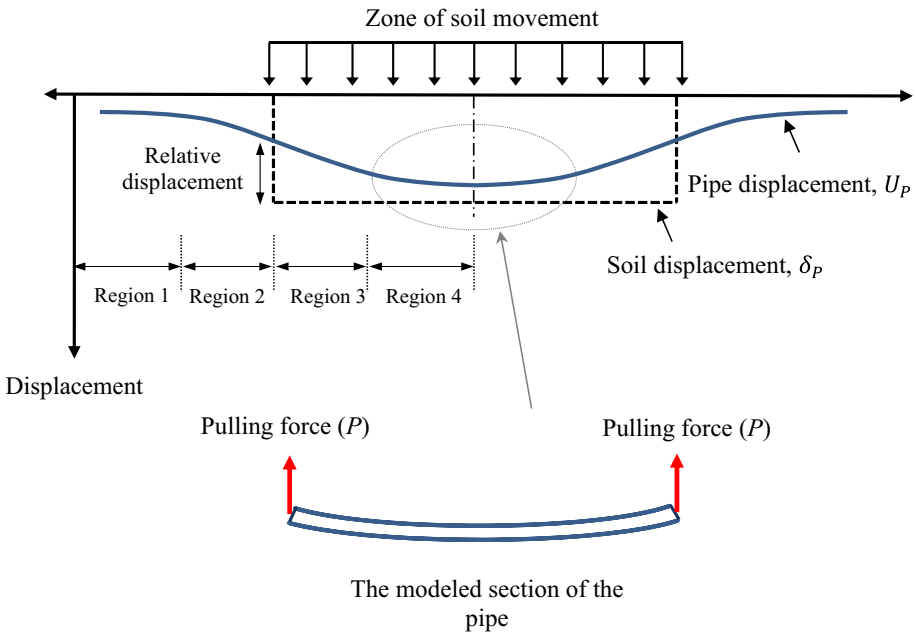

Fig. 2 A schematic of the displacement profiles of the soil and the pipe under lateral movement

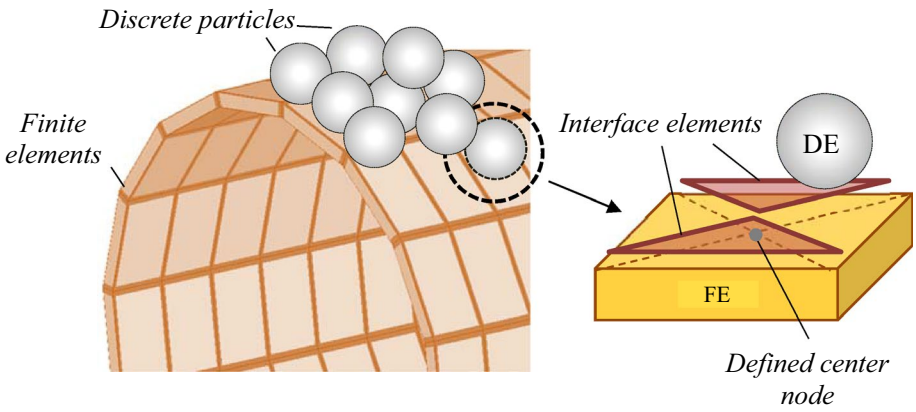

Fig. 3 The coupled FE-DE model showing the interface elements

Table 1 Properties of the backfill based on laboratory and simulated triaxial test

Parameter	Values from laboratory triaxial test [41]	Values from the simulated triaxial test
Specific gravity	2.73	–
Young's modulus, E_i (MPa)	41	36
Unit weight (kN/m^3) at D_r = 75%	16.5	–
Internal friction angle ϕ	45°	45°
Cohesion (kPa)	0	0
Poisson ratio, υ	0.30	0.28
Porosity, n	0.41	0.41

Numerical Model

The coupled FE-DE model is created based on the experiments reported by Weerasekara [34]. A polyethylene pipe 1.5 m in length buried under 0.6 m of Fraser river sand is pulled laterally while recording the pipe deformation and pulling force. Table 1 shows the properties of the backfill material used in the experiment. The numerical model is generated following the procedure used in the experiment as summarized in the following paragraph.

The Fraser River sand used in the experiment, with relative density of 75%, is modelled using spherical particles following the same particle size distribution of the granular material. As it is numerically challenging to model the exact diameters of sand particles, upscaling is employed to maintain computational feasibility. Yang et al. [35] examined the key factors controlling the strength and deformability of 2D models and concluded that the macroscopic properties of the model such as Young's modulus and Poisson's ratio are sensitive to the ratio between the shortest sample length (L) to the average of the particle diameters (d). It was found that, for 2D models, these properties tend to stabilize for L/d ratio of about 30. Ding et al. [36] examined particles with L/d ratios that range from 10 to 50. Results indicated that Young's modulus decreased with the increase in L/d ratio from 10 to 20 with very little change beyond L/d of about 20. Given the size of the 3D model in this study, particle sizes have been increased by a factor of 30. This corresponds to particle diameters that range from 2.4 mm to 9.6 mm and L/d ratio that ranges from about 15 to 47. Figure 4 presents the particles size distributions of both Fraser River sand and the discrete particles.

To determine the optimum model dimensions, 3D finite-element study is first conducted on a box of a width Y ($Y = L_1 + L_2$) and a pipe length of 1.5 m. The pipe is placed at a distance (Z) from the base (see Fig. 5). The burial depth ($H = 0.6$ m) is kept the same as that used in the experiment. Figure 6a, c presents the results of the finite element analysis. It is found that, for a displacement of 30 mm, the pulling force is affected if L_1 is less than 0.3 m, L_2 is less than 1.2 m and Z is less than 0.25 m. Therefore, the optimum dimensions of the model are chosen as 1.5 m ×1.5 m × 0.85 m (Fig. 7a).

Radius expansion method [37] is used to generate the discrete particles. It is reported by O'Sullivan [38] that this approach leads to creating a specimen with isotropic stress state. A set of non-contacting spherical particles is generated following the particle size distribution, as presented in Fig. 4. Spheres occupying the pipe circumferences are deleted and the radius of the spheres are incrementally increased to reach a porosity to 0.41 that represents that of the soil used in the experiment. Gravity is then applied to the model to reach static equilibrium. The final 3D soil specimen that consists of 345,000 spherical particles is presented in Fig. 7a. A snapshot depicting the pipeline and the surrounding soil is shown in Fig. 7b, confirms the adequacy of the particles sizes to model the soil–pipe interactions.

The MDPE pipe (length 1.5 m, diameter 114 mm and a wall thickness 10.5 mm) is modelled using 8-noded brick elements. Anderson [39] and Weerasekara [34] reported the stress–strain behaviour of the used MDPE obtained using compression and axial pullout tests and the results are presented in Fig. 8a. In addition, the non-linear hyperbolic

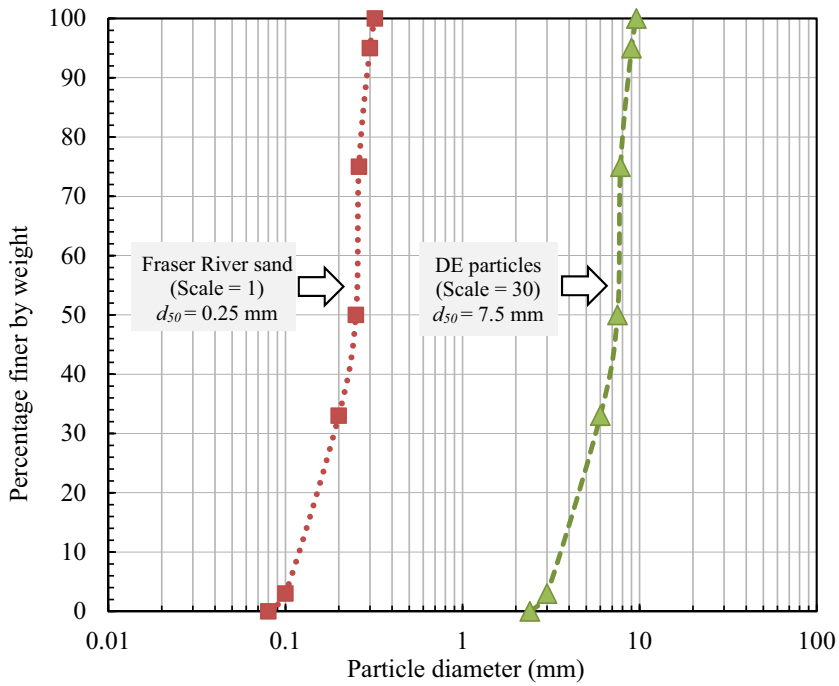

Fig. 4 Particle size distribution of the Fraser River Sand and the up-scaled discrete elements

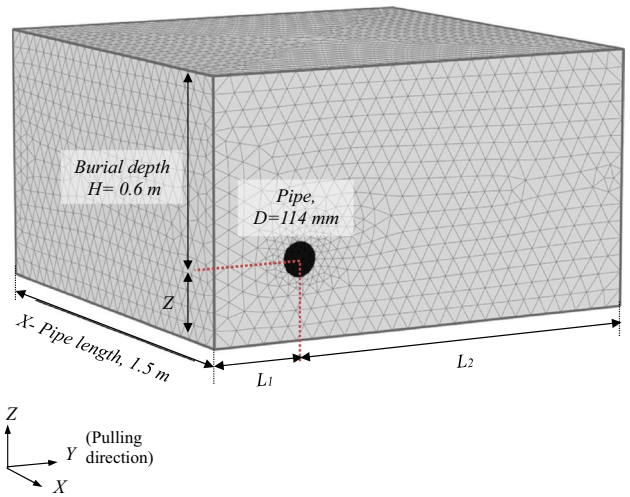

Fig. 5 Three-dimensional finite element model used to study the effect of model dimensions

model proposed by Konder [40] is also shown. The hyperbolic model is expressed by

$$\sigma = E_i\left(\frac{\varepsilon}{1+\eta\varepsilon}\right) \tag{5}$$

where σ and ε are the stress and strain, respectively. The initial Young's modulus (E_i) and η are functions of the strain rate and temperature. It is found that E_i of 645 MPa and η of 30 are required to match the experimental data reported by [34] and [39]. Given the small level of non-linearity obtained using both experiment and analytical solutions at small strain level, a simplified linear–elastic response with a Young's modulus of 550 MPa is assumed for the MDPE pipe. This assumption is considered reasonable as the maximum recorded strain is around 0.5%. Figure 8b confirms the agreement between the response of hyperbolic model and linear-elastic for the selected range of strains in the MDPE pipe. The pipe model, which comprises 1088 solid elements and 4352 interface elements, is presented in Fig. 9.

Modeling the Laboratory Experiment

Input parameters required for the discrete element analysis are obtained by calibration of the modelled particles using triaxial test results. Karimian [41] performed a number of triaxial tests on Fraser River sand under different confining stresses. The triaxial test specimen used in the analysis is created following the same particle size distribution used in the experiment. The details of the calibration procedure were reported by Meidani et al. [17]. The properties of the Fraser River sand based on laboratory and simulated triaxial tests conducted at 25 kPa confining stress are presented in Table 1. For the reported range of confining pressure [41], the sand exhibited initial elasticity, and then slightly hardened to reach a peak strength at axial strain that ranges from 3 to 6%. Other details related to shear banding and post-peak response of the tested samples are not investigated in this study. The analysis of the triaxial test showed overall agreement between the calculated and measured values, which

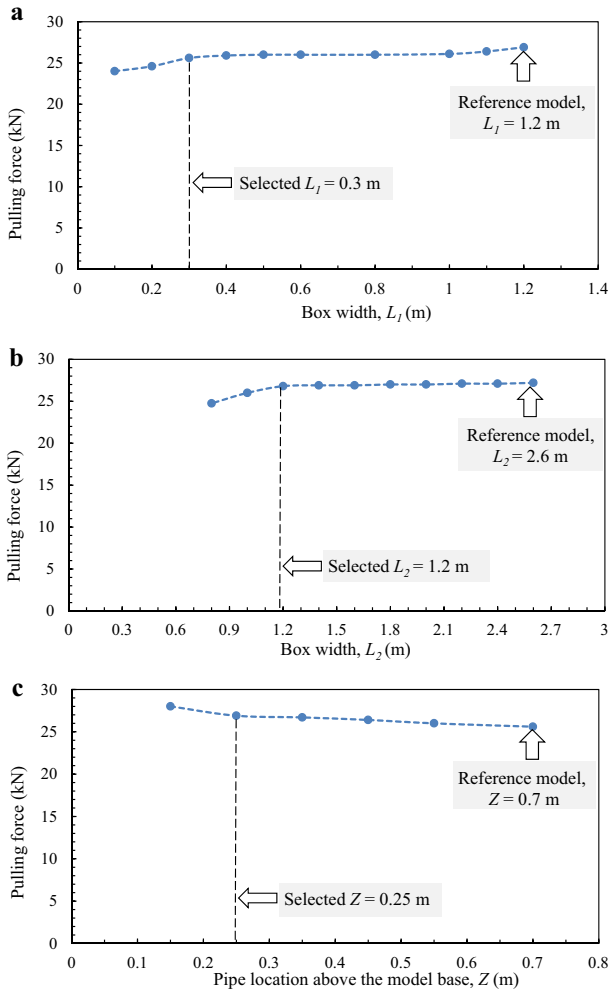

Fig. 6 Effect of model dimensions on pulling force: (**a**) L_1; (**b**) L_2; (**c**) Z

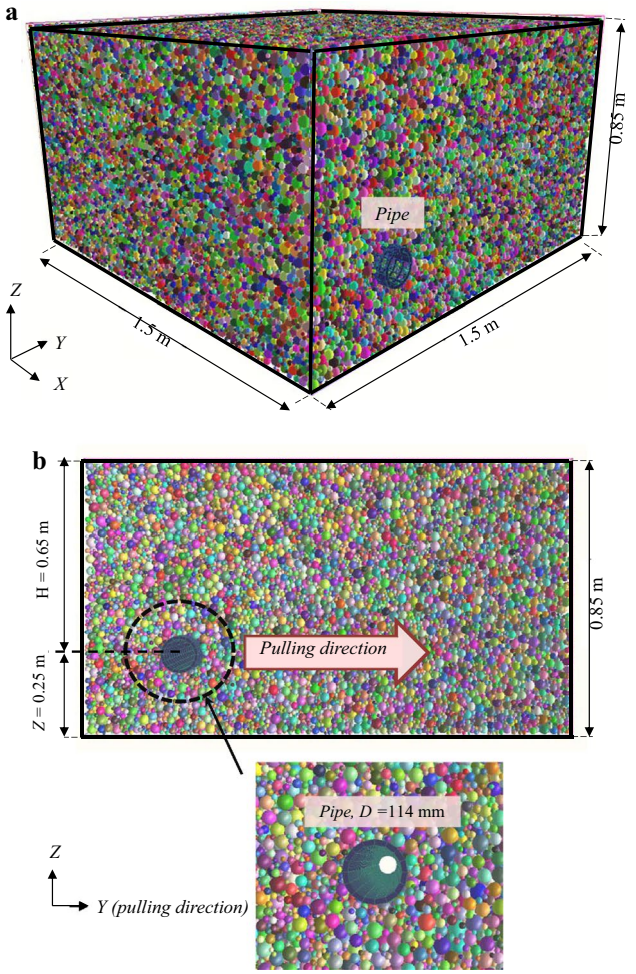

Fig. 7 The DE model: (**a**) 3D view of the pipe and the surrounding particles; (**b**) close view of the pipe

confirmed the suitability of the particle assembly in capturing the behaviour of the granular material. A summary of the input parameters used in the analysis is given in Table 2.

The coupled soil-pipe model is created and the input parameters presented in Table 2 are assigned to both the finite and discrete elements. No friction was considered along the vertical walls to follow the boundary conditions of the experiment [34]. A parametric study is conducted to evaluate the effect of the interface element properties (modulus and interface friction angle) on the test results. It is found that the changes in interface friction angle have little effects on the pulling force. Hence, a friction angle similar to that of the particles was adopted for the interface elements. The interface modulus, however, was found to have an effect on the response of the pipe. Increasing the modulus of the interface element resulted in an increase in the force required to move the pipe. Interface material modulus of about 500 MPa was found to correspond to a pipe response consistent with the experimental values. The properties of the interface elements are presented in Table 2.

The MDPE pipe is pulled laterally following a displacement control approach. Lateral displacement was applied to the pipe ends to simulate the conditions in region 4 (Fig. 2). This is consistent with the conditions used in the experiment as the pipe was clamped at the ends to ensure uniform displacement application at the pulling locations. The lateral pulling continued until a displacement of 65 mm is reached and the pulling force became constant. The relationship between the pulling force and the lateral displacement is depicted in Fig. 10. It should be noted that the pulling force shown in this figure is for one end of the pipe. The results

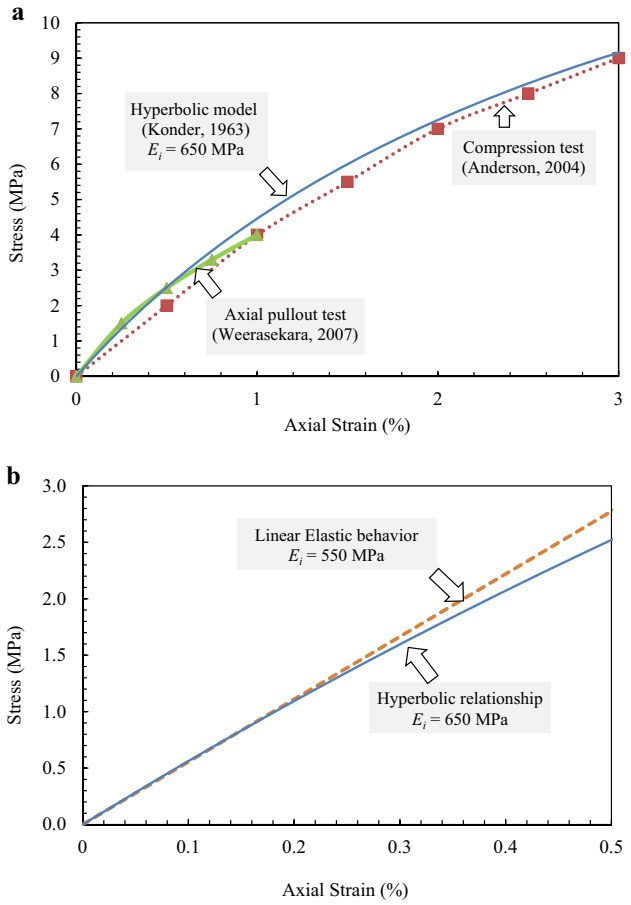

Fig. 8 **a** Experimental stress–strain response of the MDPE vs. the hyperbolic model; (**b**) comparison between linear elastic and hyperbolic models at small strain

of the analysis are found to be in agreement with the measured values and the peak lateral force (P_u) is estimated as 8.1 kN. The maximum difference between the calculated and measured results is about 15% at a lateral displacement of 10 mm. As the peak lateral force (soil lateral resistance) is of paramount importance in this study, and given the simplified nature of the analysis, the results of the coupled analysis are considered to be acceptable.

Results and Discussion

Response of the Pipe

The lateral deformation of the MDPE pipe in the *Y* direction as a function of end displacements (U_y) of 5, 20, 40 and 65 mm are plotted in Fig. 11a. The largest pipe displacement occurs at the edges and decreases rapidly towards the centre. This can be attributed to the pipe response to the applied load at the pulling location and the relative flexibility of the pipe material. This is in contrast to rigid steel pipes, where the pipe section moves as a rigid body within the soil domain under the applied lateral force. It is concluded from Fig. 11b that the pattern of the lateral displacement is uniform along the pipe section with no significant changes in the pipe cross section.

The distribution of the horizontal displacements within the pipe at $U_y = 65$ mm is depicted in Fig. 12. Figure 12a shows the displacement at the springlines, *A* and *B*. The horizontal displacement patterns are found to be the same for both sides of the springline and no horizontal displacement calculated at the pipe centre which means that no axial strains have developed in these areas. The lateral displacement direction indicates that the front side of the pipe is under compression, whereas the back side experiences tension. However, the maximum displacement in the backside (line *A*) is more than that at the front side (Line *B*), which indicates that ovalling has occurred in the pipe at this location. The horizontal displacement distribution shown in Fig. 12b illustrates that the pipe elongation is not constant and decreases towards the neutral axis, which confirms that the lateral soil force is carried mostly by bending.

Axial strains (ε_{xx}) along the pipe length are analysed to understand the load carrying mode of the MDPE pipe under the applied lateral movement. Figure 13 presents the axial strains along the pipe at applied displacement, U_y, of 65 mm. The strains along line *A*, which represents the back side of the pipe, is found to be positive which means that tensile strains and stresses have developed at this location. In contrast, the front side of the pipe (Line *B*) is found to be under compression. The values of strains at the diametrically opposite location of the pipe are opposite in direction but almost similar in magnitude which confirms the pipe section resists the applied force entirely by bending. This conclusion is in agreement with that of Chan and Wang (2004) that found bending stresses to develop in sections far from the abrupt differential ground movement (region 4 in Fig. 0.2).

The bending moment of the pipe can be calculated using the axial stresses obtained from the finite element analysis. Figure 14 presents the calculated bending moments (M_z) at three different pipe displacements. It was found that the maximum bending moment occurs close to the pipe edges at the location of the maximum relative soil-pipe displacement and decreases rapidly toward the center of the pipe, where the relative displacement is minimum.

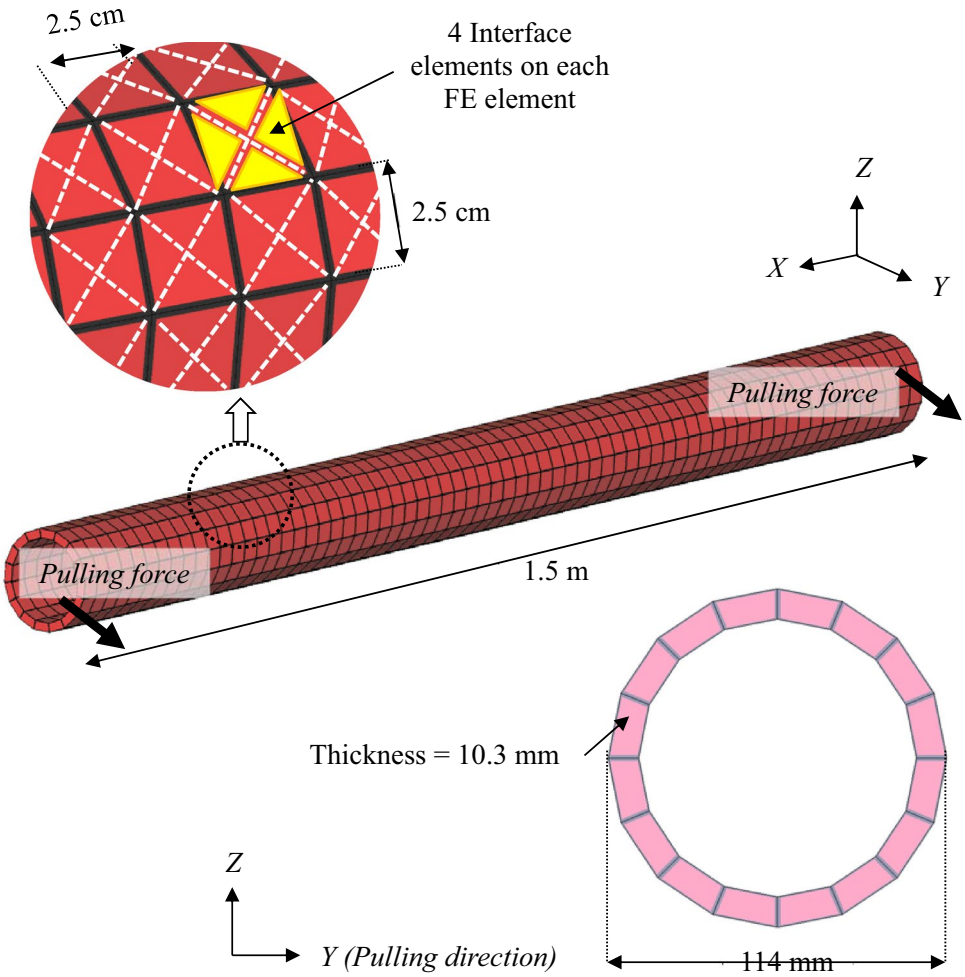

Fig. 9 Geometry of the simulated MDPE pipe and interface elements

Table 2 Parameters used in the numerical analysis

Element type	Parameter	
Discrete particles	Density	2720 kg/m^3
	Modulus, E[a]	150 MPa
	Ratio K_T/K_N, α[a]	0.7
	Friction angle, $_{micro}$[a]	45^o
	Rolling resistance coefficient, β_r[a]	0.15
	η_r[a]	1
	Damping ratio[a]	0.2
Finite elements	Young's modulus, E	550 MPa
	Poisson's ratio, υ	0.46
Interface elements	Material modulus, E	500 MPa
	Ratio K_T/K_N, α	0.7
	Micro friction angle, $_{micro}$	45^o

[a]Meidani et al. [17]

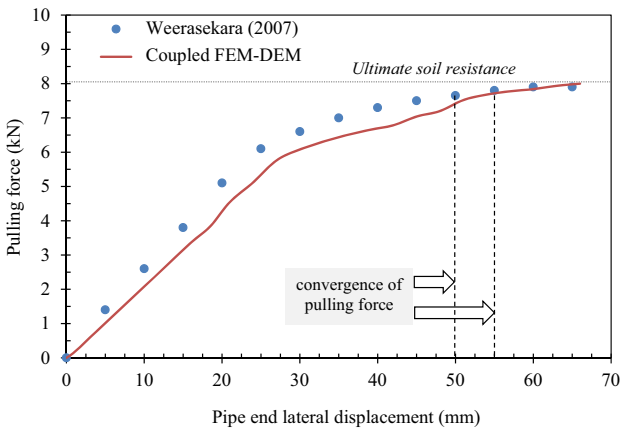

Fig. 10 Comparison between the measured and calculated responses of the pipe

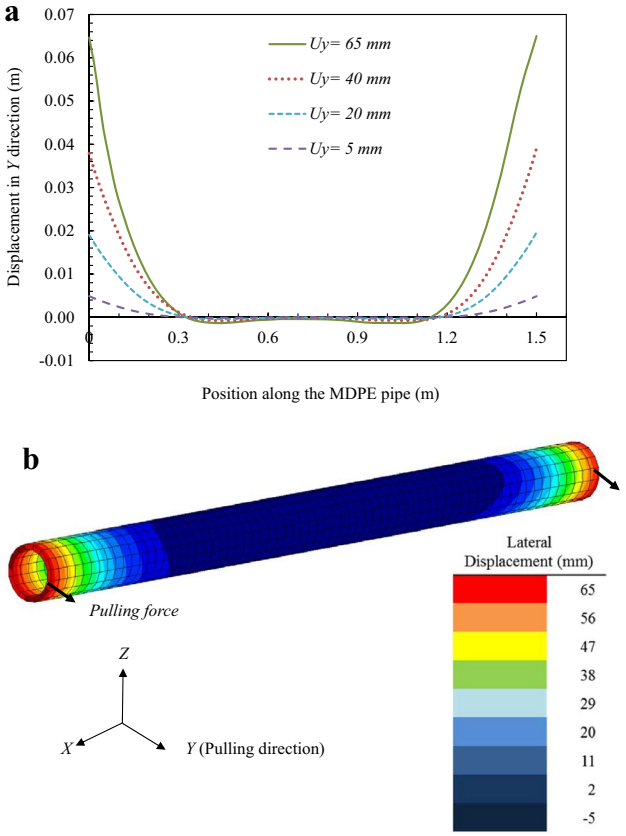

Fig. 11 Lateral displacement along the pipe length, (**a**) for different applied displacements; (**b**) at maximum displacement of U_y=65 mm pipe

Pulling Resistance

As mentioned in the previous sections, Eq. (2). is generally used to estimate the peak lateral soil load induced on pipes buried in granular soils. The term N_q in this equation is the capacity factor and researchers used different approaches to determine a suitable N_q value based on empirical solutions considering burial depth, pipe diameter and the friction angle of the soil. Less emphasis is placed on the pipe stiffness in the equation. This implies that, two pipes of different materials (e.g., steel and MDPE) and of the same diameter buried at the same depth, are expected to carry the same maximum lateral soil force. In this section, the results of the coupled analysis are compared with different solutions to calculate the peak force for laterally loaded pipes in sand. The selected studies [27, 42, 43] are based on Hansen's solution [26] and Table 3 compares the numerical results with the above methods. It should be noted that, the numerically calculated value of P_u is obtained by plotting the applied force against the lateral displacement, as illustrated in Fig. 10. It is found, based on Table 3, that the above solutions significantly overestimate the ultimate soil force. Rowe and Davis [43] and ASCE [27] solutions are found to be the closest to the numerical solution. ALA [25] and Audibert & Nyman [42] recommendations show significantly different results. Karimian [41] performed a lateral loading test on a steel pipe located in sand and reported that O'Rouke's chart [28], which is recommended by ASCE [27] predicted reasonable ultimate force values. The ALA [25] formulation, on the other hand, produced forces that are significantly higher than those calculated in this study.

Example: to illustrate the difference between the predicted ultimate lateral resistances calculated using Eq. 2 and that obtained numerically, assume $\gamma = 16$ kN/m^3, $H = 0.65$ m, $D = 0.114$ m and $N_q = 16$. The calculated ultimate lateral resistance using the closed-form solution $P_u = \gamma \times H \times N_q \times D$ is about 19 kN, which is significantly larger than 8 kN predicted using the proposed model.

Soil Response to Pipe Movement

Particle displacements can be used to better understand the response of the soil domain around the pipe. Figure 15 presents a side view that depicts particle displacements within the test box at lateral displacement of 65 mm. It is found that particles close to the pipe move in the horizontal as well as in the upward direction which creates a passive soil zone in front of the pipe and a shear failure path within the soil. The creation of passive wedge is found to be non-uniform along the pipe length which is in contrast with observations made for rigid steel pipe [41]. It can be concluded that MDPE pipes do not behave as rigid element as compared to steel pipes and only a limited segment of the pipe will reach the ultimate lateral force. It should be noted that the slight upward movement of the pipe during lateral loading is attributed to the limited burial depth in the experiment. The upward movement could be, indeed, more restricted if additional surcharge pressure is applied at the surface or if the pipe is installed at a greater depth.

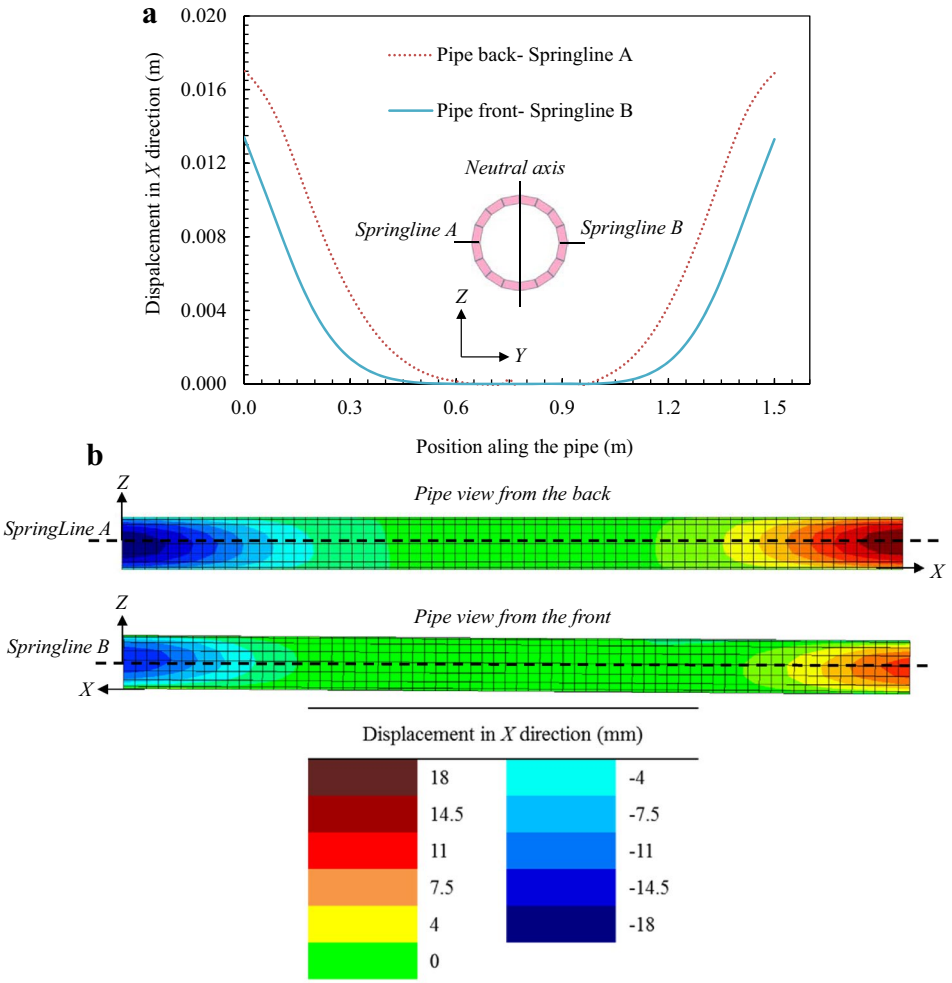

Fig. 12 Axial displacement along the pipe at applied lateral displacement U_y of 65 mm

Conclusions

In this study, the interaction of dense granular soil and MDPE pipe under lateral soil movement is evaluated using coupled finite-discreet element framework. The pipe structure is modeled using finite elements, whereas the soil particles are modeled using discrete elements. The soil domain is generated following the particle size distribution and density of the Fraser River sand used in the experiments. A calibration procedure is used to determine the micro scale parameters of the particles. The lateral force is applied to the pipe and the response, including displacements, strains and bending moments, is calculated. The ultimate lateral force is compared with the experimental results, as well as some of the commonly used solutions. In addition, the movement of the particles around the pipe is examined. The conclusions of this study are summarized below:

1. Buried MDPE pipes in dense sand subjected to lateral ground movement carry the applied load via a combination of bending and tensile strains. However, the pipe sections far from the abrupt displacement zone carry loads mostly by bending.

2. The relative soil–pipe movement, for the case of MDPE pipes under lateral loads, differs from that experienced by pipes under axial loading. The relative movement is generally non-uniform and increases from the centre of the displaced zone to maximum value towards the pipe alignment.
3. The calculated ultimate lateral load on the MDPE pipe is found to be smaller than that obtained using the available closed-form solutions. This could be attributed to the fact that these methods were mostly developed for rigid pipes. Further analysis is needed for a wider range of soil and pipe parameters to confirm these findings.

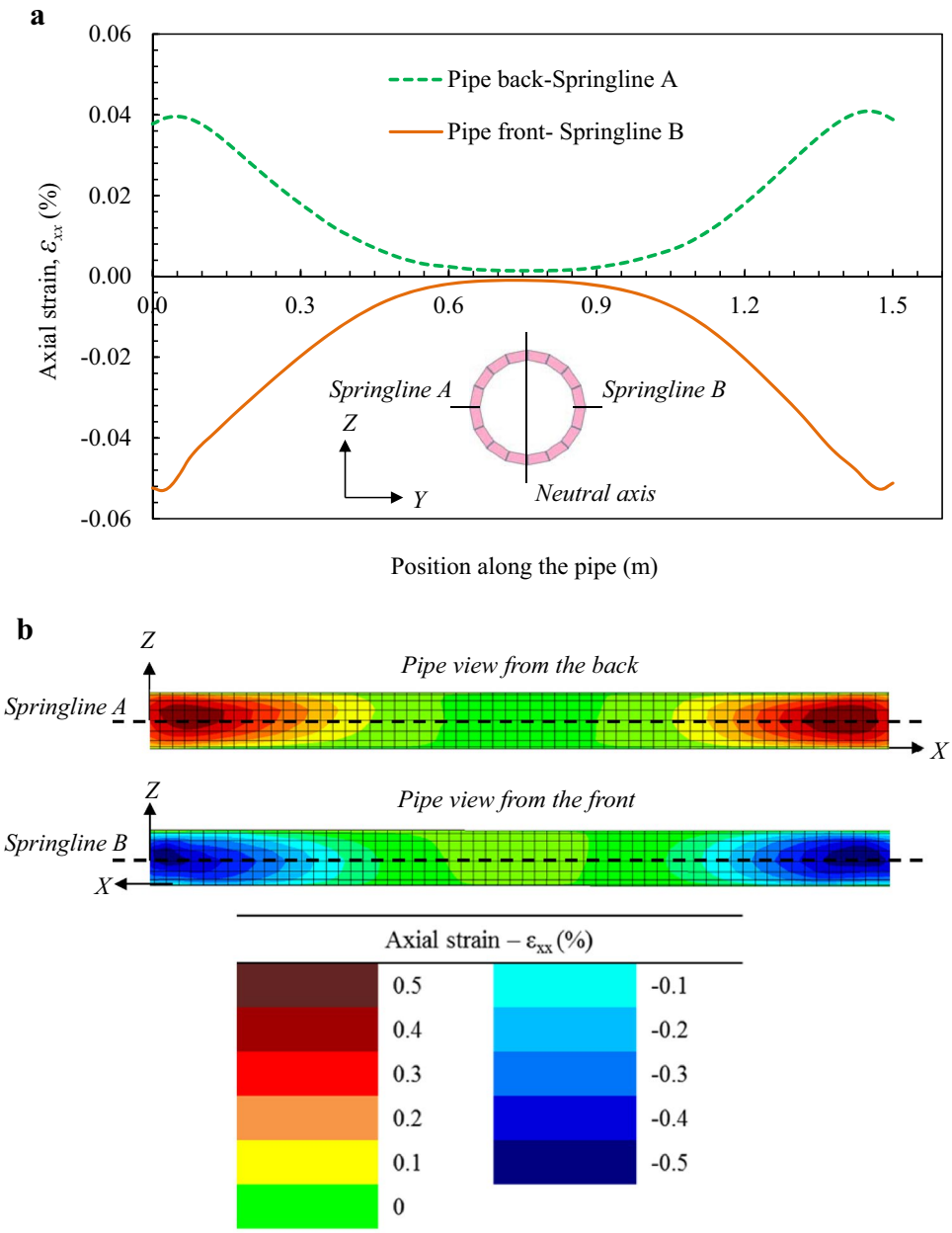

Fig. 13 Axial strain along the pipe at U_y of 65 mm

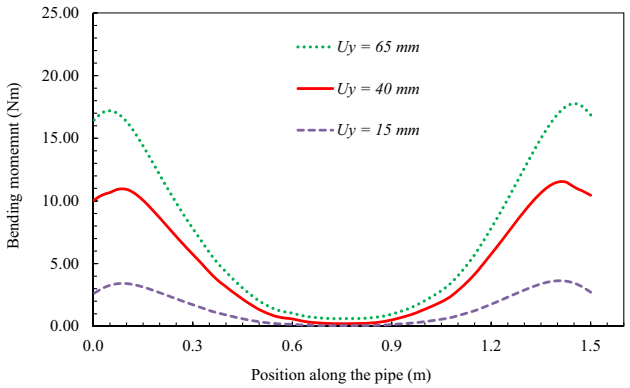

Fig. 14 Bending moment (M_z) along the pipe for different applied displacements

4. It should be noted that the results presented in this study focused on the bending response of MDPE pipes under relative soil movement. The presented results are based on analysing a limited section of the buried pipe using simplified linear elastic model that did not consider the possible nonlinear behaviour, strain rate effect, and time-dependent response of the MDPE material. In addition, granular material used in the large scale experiment is represented using scaled-up particles to keep the computational cost manageable. Further investigations are also needed to study the combined axial and bending behaviour of the buried pipe under lateral loading.

Table 3 Comparison between different methods used to calculate the ultimate lateral pressure of loaded pipes in granular material

Reference	N_q	P_u (kN)	Comments
FE-DE analysis (current study)	–	8.1[a]	Laterally loaded MDPE pipe
Rowe and Davis [43]	15	26.7	Anchor in sand
ASCE [27]—based on [3]	16	28.5	Laterally loaded steel pipe
Wilson-Fahmy et al. [42]	25	44.5	Polymeric geogrids in pullout

[a]The ultimate soil resistance, P_u, is obtained, as illustrated in Fig. 10

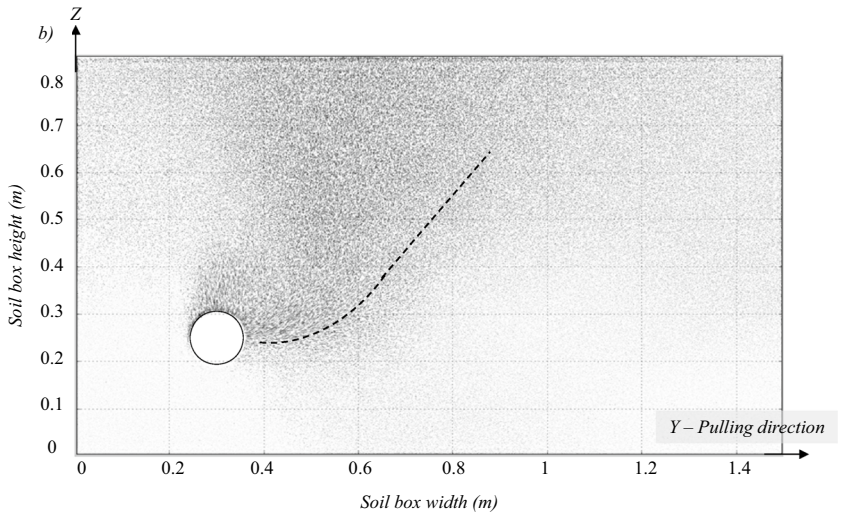

Fig. 15 Side view showing the displacement field within the soil domain at U_y of 65 mm

References

1. NRC (2016) Natural Resources Canada, https://www.nrcan.gc.ca/energy/infrastructure/18856. Accessed Jan 15 2018.
2. Ovesen NK (1964) Anchor slabs, calculation methods and model tests, Bulletin No. 16, The Danish Geotechnical Institute, Copenhagen, Denmark.
3. Trautmann CH, O'Rourke TD (1983) Behaviour of pipe with dry sand under lateral and uplift loading, geotechnical engineering report 83–7. Cornell University, Ithaca
4. Konuk I, Hilips R, Urley S, Paulin MJ (1999) Preliminary ovalization measurement of buried pipelines subject to lateral bending. Submitted to 18th offshore mechanics and arctic engineering conference, St. John's, NF.
5. Weerasekara L, Wijewickreme D (2008) Mobilization of soil loads on buried, polyethylene natural gas pipelines subject to relative axial displacements. Can Geotech J 45:1237–1249
6. Daiyan N, Kenny S, Phillips R, Popescu R (2011) Investigating pipeline-soil interaction under axial–lateral relative movements in the sand. Can Geotech J 48(11):1683–1695
7. Robert DJ, Soga K, O'Rourke TD, Sakanoue T (2016) Lateral load-displacement behaviour of pipelines in unsaturated sands. J Geotech Geoenviron Eng 142(11):04016060
8. Meidani M, Meguid MA, Chouinard LE (2018) Estimating earth loads on buried pipes under axial loading condition: insights from 3D discrete element analysis. Int J Geo-Eng 9(1):1–20
9. Guo PJ, Stolle DFE (2005) Lateral pipe-soil interaction in sand with reference to scale effect. J Geotech Geoenviron Eng ASCE 131(3):338–349
10. Xie X (2008) Numerical analysis and evaluation of buried pipeline response to earthquake-induced ground fault rupture. Ph.D. thesis, Rensselaer Polytechnic Institute, New York.
11. Roy K, Hawlader B, Kenny S, Moore ID (2015) Finite element modeling of lateral pipeline–soil interactions in dense sand. Can Geotech J 53(3):490–504
12. Zhang J, Zheng L, Chuanjun H (2016) Mechanical behaviour analysis of the buried steel pipeline crossing landslide area. J Pressure Vessel Technol 138(5):051702
13. Naeini SA, Mahmoudi E, Shojaedin MM, Misaghian M (2016) Mechanical response of buried high-density polyethylene pipelines under normal fault motions. KSCE J Civ Eng 20(6):2253–2261
14. Cundall PA, Strack OD (1979) A discrete numerical model for granular assemblies. Geotechnique 29(1):47–65
15. Han K, Owen DRJ, Peric D (2002) Combined finite/discrete element and explicit/implicit simulations of peen forming process. Eng Comput 19(1):92–118
16. Tran VDH, Meguid MA, Chouinard LE (2014) Three-dimensional analysis of geogrid-reinforced soil using a finite-discrete element framework. Int J Geomech 15(4):04014066
17. Meidani M, Meguid MA, Chouinard LE (2017) Evaluation of soil-pipe interaction under relative axial ground movement. J Pipeline Syst Eng Practice 8(4):04017009
18. Lin YL, Zhang MX, Javadi AA, Lu Y, Zhang SL (2013) Experimental and DEM simulation of sandy soil reinforced with H-V inclusions in plane strain tests. Geosynthetics Int 20(3):162–173
19. McDowell GR, Harireche O, Konietzky H, Brown SF, Thom NH (2006) Discrete element modelling of geogrid-reinforced aggregates. Proc ICE-Geotech Eng 159(1):35–48

20. Fakhimi A (2009) A hybrid discrete–finite element model for numerical simulation of geomaterials. Comput Geotech 36(3):386–395
21. Villard PB, Chevalier B, Hello L, Combe G (2009) Coupling between finite and discrete element methods for the modeling of earth structures reinforced by geosynthetic. Comput Geotech 36(5):709–717
22. Dang HK, Meguid MA (2013) An efficient finite-discrete element method for quasi-static nonlinear soil-structure interaction problems. Int J Numer Anal Meth Geomech 37(2):130–149
23. Tran VDH, Meguid MA, Chouinard LE (2013) A finite-discrete element framework for the 3D modeling of geogrid-soil interaction under pullout loading conditions. Geotext Geomembr 37:1–9
24. Meidani M, Meguid MA, Chouinard LE (2018) A finite-discrete element approach for modeling polyethylene pipes subjected to axial ground movement. Int J Geotech Eng. https://doi.org/10.1080/19386362.2018.1483812
25. ALA (2001) Guideline for the design of buried steel pipe. American Lifeline Alliance (ALA). www.americanlifelinealliance.org/Product_new3.htm. Accessed 15 June 2018
26. Rajani BB, Robertson PK, Morgenstern NR (1995) Simplified design methods for pipelines subject to transverse and longitudinal soil movements. Can Geotech J 32(2):309–323
27. ASCE (1984) Guidelines for the seismic design of oil and gas pipeline systems. Committee on Gas and Liquid Fuel Lifelines. American Society for Civil Engineering (ASCE), New York
28. O'Rourke TD (1988) Critical aspects of soil-pipeline interaction for large ground deformation. In: Proceedings, 1st Japan-US Workshop on liquefaction, large ground deformation and their effects on lifelines, association for development of earthquake prediction, Japan, 118–126.
29. Hansen BJ (1961) The ultimate resistance of rigid piles against transversal forces. Bulletin 12, Danish Geotechnical Institute, Copenhagen, Denmark.
30. Chan PDS, Wong RCK (2004) Performance evaluation of a buried steel pipe in a moving slope: a case study. Can Geotech J 41(5):894–907
31. Dang HK, Meguid MA (2010) Algorithm to generate a discrete element specimen with predefined properties. Int J Geomech 10(2):85–91
32. Kozicki J, Donzé VF (2008) A new open-source software developed for numerical simulations using discrete modeling methods. Comput Methods Appl Mech Eng 197:49–50
33. Smilauer V et al. (2010) Yade documentation. The Yade project 2010. https://yade-dem.org/doc/Yade.pdf. Accessed 15 June 2018
34. Weerasekara L (2007) Response of buried natural gas pipelines subjected to ground movements. M.A.Sc. thesis, Department of Civil Engineering, University of British Columbia, Vancouver, B.C.
35. Yang B, Jiao Y, Lei S (2006) A study on the effects of microparameters on macroproperties for specimens created by bonded particles. Eng Comput 23(6):607–631
36. Ding X, Zhang L, Zhu H, Zhang Q (2014) Effect of model scale and particle size distribution on PFC3D simulation results. Rock Mech Rock Eng 47:2139–2156
37. Itasca (2004) PFC 2D 3.10 Particle Flow Code in two dimensions, theory and background volume (third ed.). Minneapolis, Minnesota.
38. O'Sullivan C (2011) Particulate discrete element modeling, a geomechanics perspective. Spon Press, London
39. Anderson C (2004) Soil–pipeline interaction of polyethylene natural gas pipelines in sand. M.Sc. thesis, Department of Civil Engineering, University of British Columbia, Vancouver, B.C.
40. Konder RB (1963) Hyperbolic stress-strain response: cohesive soils. J Soil Mech Foundations Division ASCE 89(SM1):115–143
41. Karimian H (2006) Response of buried steel pipelines subjected to longitudinal and transverse ground movement. Ph.D. thesis, Department of Civil Engineering, The University of British Columbia, Vancouver, B.C.
42. Audibert JME, Nyman KJ (1977) Soil restraint against horizontal motion of pipes. J Geotech Eng Div ASCE 103(GT10):1119–1142
43. Rowe RK, Davis EH (1982) The behaviour of anchor plates in sand. Geotechnique 32(1):25–41